ELSEVIER

Journal of Nuclear Materials 283–287 (2000) 773–777

journal of nuclear materials

www.elsevier.nl/locate/jnucmat

Atomistic simulation of stacking fault tetrahedra formation in Cu

B.D. Wirth *, V. Bulatov, T. Diaz de la Rubia

Lawrence Livermore National Laboratory, Chemistry and Materials Science Directorate, P.O. Box 808, L-353, Livermore, CA 94551, USA

Abstract

Atomistic simulations based on the embedded atom method (EAM) are used to model the formation of stacking fault tetrahedra (SFT) in face centered cubic (fcc) Cu. SFTs are observed in fcc metals following both irradiation and plastic deformation and have significant impact on defect accumulation and microstructural evolution of the irradiated material. Many authors have proposed SFT formation mechanisms; however, a concise atomistic view is lacking. Starting from the vacancy-rich regions produced in high-energy displacement cascades, we have performed molecular dynamics (MD) simulations at a range of temperatures and observed SFT formation. In this work, we provide an atomistic picture of SFT formation.

1. Introduction

Following the discovery of stacking fault tetrahedra (SFT) in quenched gold by Silcox and Hirsch [1], SFT have been observed in face centered cubic (fcc) materials following irradiation, quenching from high temperature and plastic deformation [1–7]. Silcox and Hirsch [1] proposed the following mechanism (see Fig. 1) for SFT formation; a vacancy disc nucleates on a $\{1\,1\,1\}$ plane and collapses to form a loop bounded by Frank partial dislocations $(a/3\langle 1\,1\,1\rangle)$. Each of the Frank partials dissociates to form a low energy stair-rod partial $(a/6\langle 1\,0\,1\rangle)$ and a Shockley partial $(a/6\langle 1\,2\,1\rangle)$ dislocation. An SFT then forms as the Shockley partials glide towards the apex of the tetrahedron formed by three intersecting $\{1\,1\,1\}$ planes and the original loop $\{1\,1\,1\}$ plane. The reaction of Shockley partials at each intersection of $\{1\,1\,1\}$ planes produces stair-rod partial dislocations. The resulting SFT has four triangular $\{1\,1\,1\}$ planes bounded by six stair-rod partial dislocations.

Several authors have proposed SFT formation mechanisms, three of which have been reviewed by Jossang and Hirth [8]. Those mechanisms are briefly summarized as: (i) vacancy clustering and dislocation glide (the Silcox–Hirsch mechanism discussed in the previous paragraph); (ii) direct vacancy clustering in which a tri- or tetra-vacancy acts as an SFT nucleus that can grow by the absorption of vacancies at jogs on truncated SFTs; and (iii) dislocation glide which produces SFTs by the cross-slip of extended dislocations at super-jogs [8].

Following high-energy particle irradiation, the observed mean SFT size remains approximately constant over a wide irradiation dose and temperature range [4,5]. For example, in Cu the mean SFT size is 2.5 ± 0.5 nm at temperatures between 20°C and 100°C and for doses between 10^{-4} and 10^{2} dpa [4,5]. Molecular dynamics (MD) simulations of displacement cascade evolution in Cu and other fcc metals has revealed the formation of large vacancy loops, but SFT formation has not been predicted (see for example [9]). Many computer simulation studies have modeled vacancy cluster and SFT properties in Cu [10–13] and SFT formation under irradiation [14,15]. However, a concise atomistic view of SFT formation under irradiation is still lacking. This paper reports a comprehensive atomistic simulation of SFT formation in Cu with particular emphasis on the formation mechanism, starting from both triangular vacancy platelets and vacancy configurations obtained from high-energy displacement cascades.

* Corresponding author. Tel.: +1-925 424 9822; fax: +1-925 423 7040.

E-mail address: wirth4@llnl.gov (B.D. Wirth).

0022-3115/00/$ - see front matter
PII: S0022-3115(00)00262-2

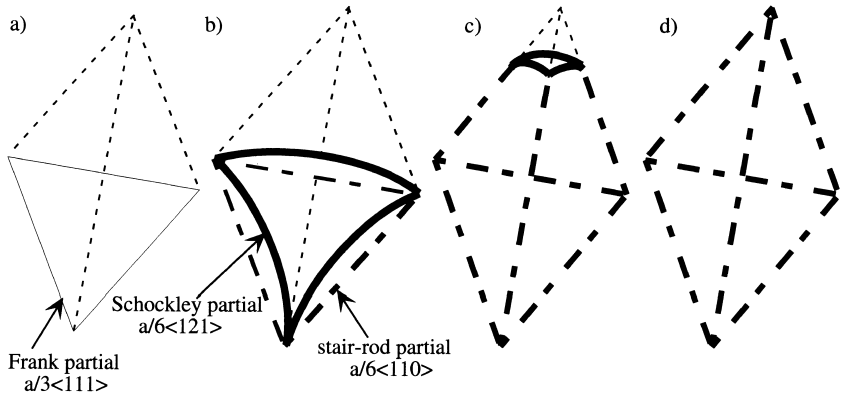

Fig. 1. Dislocation viewpoint of SFT formation, as proposed by Silcox and Hirsch [1,8].

2. Simulation methodology

MD simulations of SFT formation in Cu were performed using the MDCASK code [16] and an embedded atom method (EAM) potential [17,18]. All of the simulations presented here used periodic boundary conditions and constant volume with a supercell that contained $32000 - N$ atoms, N is the number of vacancies. In all cases, the simulation cell was first equilibrated for 25 ps at temperatures from 100 to 300 K and then N atoms were removed in the central region of the supercell to introduce the desired vacancy cluster configuration. Triangular platelets and vacancy cluster configurations obtained from high energy MD displacement cascades [19] were used as starting vacancy configurations.

3. Results and discussion

MD simulations of SFT formation have been performed starting from triangular vacancy platelets containing 10–190 vacancies and cascade vacancy configurations containing 32 and 68 vacancies. In this work, we only report results for the triangular platelet containing 55 vacancies, corresponding to an SFT edge length of 2.55 nm, and the 68-vacancy cascade configuration; the other results will be reported elsewhere [20]. Fig. 2 shows five snapshots from a MD simulation at 100 K in which the 55-vacancy triangular platelet first relaxes to a Frank loop and subsequently transforms to an SFT. Fig. 2(a) shows a [1 0 1] projection of all of atoms within a region encompassing the SFT; Fig. 2(b) and (c) show the atoms with high potential energy in [1 0 1] and $[1\,1\,\bar{1}]$ projections, respectively. The times denote the elapsed time since the introduction of the vacancies. Note, the final frame (denoted by 1.0 ps, static) shows the configuration 1 ps after introduction of the vacancy platelet and has been quenched to 0 K to remove thermal disorder and provide a cleaner picture of the SFT structure. Viewing the high-energy atoms provides a clear picture of the dislocation core structure.

In the first 0.5 ps following introduction of the vacancy platelet on a $(1\,1\,\bar{1})$ plane, the two neighboring $(1\,1\,\bar{1})$ planes collapse towards the vacant triangular disc to form a Frank loop, as evidenced in Fig. 2(b). SFT formation at 100 K occurs in the next 0.5 ps. From an atomistic perspective (Fig. 2(a)), SFT formation results from the collective displacement of atoms within the tetrahedron as they fall $(1\,1\,\bar{1})$ plane by $(1\,1\,\bar{1})$ plane into the hole left by the original vacancy platelet (Frank loop). The resulting structure is clearly visible as an SFT in the final frame of Fig. 2(a). The mean displacement of atoms within the SFT is $a/4\lfloor\bar{1}\,\bar{1}\,1\rfloor$. Of course, this description of collective displacements, as planes of atoms drop one by one into the original platelet, is actually a description of dislocation motion; each plane of atoms is displaced as the Shockley partials glide past.

By viewing the dislocation core structure in Figs. 2(b) and (c), we gain a dislocation perspective of SFT formation. Between 0.5 and 0.7 ps, each of the three Frank partials dissociate to form stair-rod and Shockley partials, clearly shown in Fig. 2(c) as a change in dislocation core structure. Over the next 0.3 ps, the Shockley partials glide towards the apex of the tetrahedron. The reaction of Shockley partials at intersecting $\{1\,1\,1\}$ planes produces stair-rod partial dislocations, again clearly evidenced in Fig. 2(c) by comparing the snapshots at 0.7, 0.9 and 1.0 ps. The resulting structure is a SFT bounded by six stair-rod dislocations. It is interesting to note that equal probabilities exist for formation of the Shockley partials on either side of the Frank loop during dissociation. In this case, the partials dissociated in the $[1\,1\,\bar{1}]$ direction.

Not surprisingly, both the atomistic and dislocation perspectives show that the SFT forms by the Silcox–Hirsch mechanism when started from a triangular vacancy platelet. However, an outstanding question is the

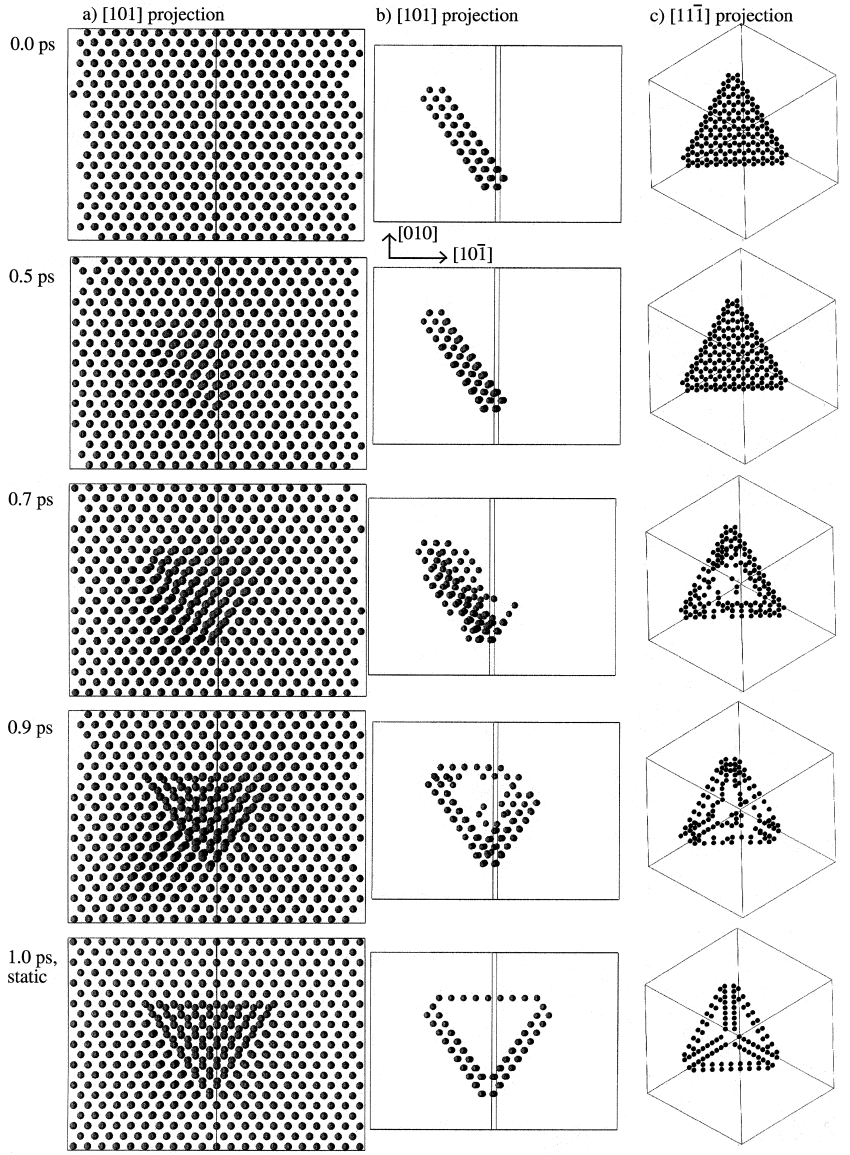

Fig. 2. MD simulation snapshots of SFT formation at 100 K from (a) [1 0 1] projection of all the atoms surrounding the SFT; (b) [1 0 1] projection of the high-energy atoms and (c) [1 1 $\bar{1}$] projection of the high-energy atoms.

mechanism by which SFTs form under irradiation. We used the same MD simulation approach to study SFT formation at 300 K, starting from the spatial vacancy arrangement obtained from displacement cascades.

Fig. 3(a) shows two perspectives of the distribution of 68 vacancies obtained from the core of a 20 keV displacement cascade in Cu, provided by Alonso and Caturla [19]. Thirty nine of the vacancies condensed during the short-term cooling of the cascade into a trapezoidal arrangement on a {1 1 1} plane. MD simulation at 300 K for 1 ps resulted in the formation of overlapping, truncated SFTs, as shown in the projections of Figs. 3(b) and (c) for all of the atoms surrounding the SFTs and the high-energy atoms, respectively. The small cluster of high-energy atoms to the lower left of the stair-rod partial dislocations bounding the SFT structure shows the position of a single vacancy. SFT formation occurred from the trapezoidal shaped vacancy platelet by the same Silcox–Hirsch mechanism, as shown in Fig. 2 for the triangular platelet, but will be presented elsewhere [20]. However, in this case, the trapezoidal shaped loop subdivided into two triangular regions, each of which dissociated on opposite sides of the original platelet. Neither of the two triangular regions was a

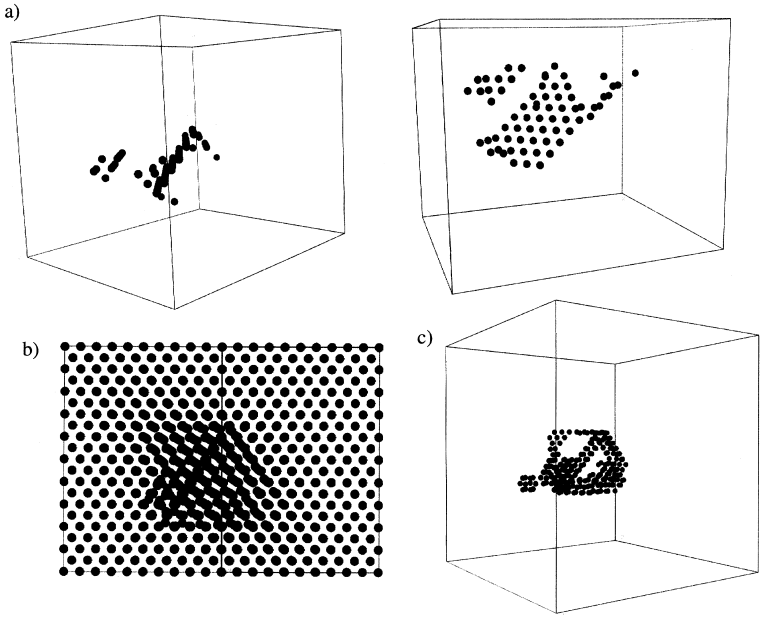

Fig. 3. (a) Spatial distribution of 68 vacancies obtained from a 20 keV displacement cascade in Cu; (b) [1 0 1] projection of all the atoms surrounding the overlapping, truncated SFTs formed at 300 K and (c) near [1 0 1] projection of the high-energy atoms.

perfect equilateral triangle and the resulting overlapping SFTs are truncated. Further, another small truncated SFT formed from the smaller vacancy platelet (on the left side of the trapezoidal loop in Fig. 3(a)), although it is not readily identifiable in Figs. 3(b) and (c). Defects such as these are commonly observed in TEM examinations [21,22].

It is important to note that the starting vacancy configuration in this simulation had already condensed to a vacancy platelet and, thus, SFT formation occurred within 1 ps at 300 K. However, in general, the vacancy structure within the cascade core following short-term cascade cooling may not consist of vacancy platelets. In that case, the time scale for SFT formation will be dependent on vacancy diffusion to first form a Frank loop (vacancy platelet) with subsequent rapid SFT formation by the Silcox–Hirsch mechanism. We cannot exclude some contribution of direct vacancy clustering to SFT formation under irradiation. However, it is difficult to rationalize a constant mean SFT size during irradiation with the amount of vacancy diffusion required for any significant fraction of SFT formation from direct vacancy clustering.

4. Conclusion

We have presented selected results from a comprehensive atomistic study of SFT formation in copper that show, for the first time, a concise, atomistic picture of SFT formation by the Silcox–Hirsch mechanism. Further, our results suggest that under irradiation, SFT formation will occur by the Silcox–Hirsch mechanism with a time scale determined by the vacancy diffusion (if any) required for vacancy platelet condensation.

Future work will focus on the energetics of SFTs, the curvature of the Shockley partials during their glide to the SFT apex and interaction between a moving dislocation and SFTs [20].

Acknowledgements

This work was performed under the auspices of the US Department of Energy and Lawrence Livermore National Laboratory under contract No. W-7405-Eng-48.

References

[1] J. Silcox, P.B. Hirsch, Philos. Mag. 4 (1959) 72.
[2] M.L. Jenkins, Philos. Mag. 29 (1974) 813.
[3] S.J. Zinkle, J. Nucl. Mater. 150 (1987) 140.
[4] Y. Dai, M. Victoria, Mater. Res. Soc. Symp. Proc. 439 (1997) 319.
[5] B.N. Singh, S.J. Zinkle, J. Nucl. Mater. 206 (1993) 212.
[6] Y. Dai, M. Victoria, Acta Mater. 45 (1997) 3495.
[7] M. Kiritani, personal communication.
[8] T. Jossang, J.P. Hirth, Philos. Mag. 13 (1966) 657.

[9] D. Bacon, T. Diaz de la Rubia, J. Nucl. Mater. 216 (1994) 275.
[10] E.J. Savino, R.C. Perrin, J. Phys. F 4 (1974) 1889.
[11] C.C. Matthai, D.J. Bacon, J. Nucl. Mater. 135 (1985) 173.
[12] M.J. Sabochick, S. Yip, N.Q. Lam, J. Phys. F 18 (1988) 349.
[13] Y. Osetsky, A. Serra, M. Victoria, S.I. Golubov, V. Priego, Philos. Mag. A 79 (1999) 2259.
[14] V.G. Kapinos, Y. Osetsky, P.A. Platanov, J. Nucl. Mater. 165 (1989) 286.
[15] K. Nordlund, F. Gao, Appl. Phys. Lett. 74 (1999) 2720.
[16] T. Diaz de la Rubia, M.W. Guinan, J. Nucl. Mater. 174 (1990) 151.
[17] S.M. Foiles, M.I. Baskes, M.S. Daw, Phys. Rev. B 33 (1986) 7983.
[18] M. Ghaly, R.S. Averback, personal communication.
[19] E. Alonso, M.J. Caturla, personal communication.
[20] B.D. Wirth, V. Bulatov, T. Diaz de la Rubia, Philos. Mag. A (to be submitted).
[21] S.J. Zinkle, personal communication.
[22] R. Schaublin, personal communication.